

# Relativistic SPH Calculations of Compact Binary Mergers

Frederic Rasio<sup>1</sup>, Joshua Faber<sup>2</sup>, Shiho Kobayashi<sup>3</sup>, and Pablo Laguna<sup>4</sup>

<sup>1</sup>*Department of Physics and Astronomy, Northwestern University, Evanston, IL 60208, USA*

<sup>2</sup>*Department of Physics, University of Illinois, Urbana, IL 61801, USA*

<sup>3</sup>*Center for Gravitational Wave Physics, Pennsylvania State University, University Park, PA 16802, USA*

<sup>4</sup>*Department of Astronomy and Astrophysics and Department of Physics, Pennsylvania State University, University Park, PA 16802, USA*

## Abstract

We review recent progress in understanding the hydrodynamics of compact binary mergers using relativistic smoothed particle hydrodynamics (SPH) codes. Recent results are discussed for both double neutron stars and black hole – neutron star binaries. The gravitational wave signals from these mergers contain a lot of information about the masses and radii of the stars and the equation of state of the neutron star fluid. For black hole – neutron star mergers, the final fate of the fluid and the gravitational wave emission depend strongly on the mass ratio and the black hole spin.

## 1 Introduction

Coalescing compact binaries containing neutron star (NS) or black hole (BH) components are the leading candidates to become the first observed sources of gravitational waves (GW). With LIGO, GEO, and TAMA all taking scientific data, and VIRGO in the commissioning stage, it is now more important than ever to develop quantitatively accurate predictions of the GW signals we expect to observe from the binary merger process. These GW signals contain crucial information about the masses, NS radii, and NS equation of state (EOS).

Calculations of binary NS coalescence have been performed for many years, beginning almost 20 years ago with studies in Newtonian gravity (see, e.g., Nakamura 1994; Rasio & Shapiro 1999; for reviews of early work). It was recognized all along, however, that general relativity (GR) must play an important role, given the strong gravitational fields and relativistic velocities involved, particularly near the end of the merging process. As a result, increasingly sophisticated gravitational formalisms have been used in combination with 3-D hydrodynamic calculations, starting with post-Newtonian (PN) treatments (Oohara & Nakamura 1992; Shibata 1997; Lombardi, Rasio, & Shapiro 1997; Faber & Rasio 2000, 2002; Ayal et al. 2001). Several recent studies were based on the PN hydrodynamics formalism developed by Blanchet, Damour & Schäfer (1990), which includes all lowest-order 1PN effects as well as the lowest-order dissipative effects from gravitational radiation reaction. Most recently, calculations have been performed in full GR, using the techniques of 3-D numerical relativity (Shibata & Uryu 2000, 2001; Shibata, Taniguchi, & Uryu 2003; Miller, Gressman, & Suen 2004). These are plagued by numerical difficulties, but allow one to address fundamentally new and important questions, such as the stability of the final merger remnant to gravitational collapse.

Unfortunately, while considerably easier to implement numerically, the PN approximation breaks down during the merger when higher-order relativistic effects grow significant. A middle ground is provided by the conformally flat (CF) approximation to GR, developed originally by Wilson and collaborators (see, e.g., Wilson, Mathews & Marronetti 1996). This approximation is used in essentially all quasi-equilibrium calculations of initial data for compact binary mergers (NS–NS, BH–NS, and BH–BH; see, e.g., Faber et al. 2002; Grandclément, Gourgoulhon, & Bonazzola 2002). It has also been used more recently for

---

<sup>1</sup>Email: rasio@northwestern.edu

<sup>2</sup>Email: jfaber@uiuc.edu

<sup>3</sup>Email: shiho@gravity.psu.edu

<sup>4</sup>Email: pablo@astro.psu.edu

full hydrodynamic merger calculations (Oechslin, Rosswog, & Thielemann 2002; Faber, Grandclément, & Rasio 2004). An overview of the latest results from Faber et al. (2004) is given in Sec. 3. The CF approximation includes much of the non-linearities inherent in GR, but reduces the Einstein field equations to a set of coupled, non-linear, elliptic equations, which can be solved numerically using well-understood, robust techniques. While this approach cannot reproduce the exact GR solution for a general 3-D matter configuration, it is exact for spherically symmetric systems, and, in practice, yields solutions that often agree closely with those calculated using full GR (Mathews, Marronetti, & Wilson 1998; Shibata & Sekiguchi 2004). Most remarkably, CF solutions for BH–BH binaries in quasi-equilibrium agree extremely well with those obtained from the most accurate, high-order PN treatment (Damour, Gourgoulhon, & Grandclément 2002).

In contrast to NS–NS merger calculations, relatively little work has been done on BH–NS mergers. Newtonian hydrodynamic calculations for a polytrope around a point mass (e.g., Lee 2001) are of limited applicability to the highly relativistic BH–NS systems. Relativistic quasi-equilibrium calculations of BH–NS binaries near the Roche limit have been performed recently by several groups (Baumgarte, Skoge, & Shapiro 2004; Ishii, Shibata, & Mino 2005). Some initial results from our own relativistic hydrodynamic study of BH–NS mergers are presented in Sec. 4. In spite of the great astrophysical importance of BH–NS binaries, our theoretical understanding of these systems lags behind that of NS–NS binaries by at least 10 years. One key question concerns the timescale of the tidal disruption and whether quasi-stable mass transfer from a NS to a BH can ever occur. This has important consequences for the detectability of the GW signal associated with the tidal disruption. This signal carries information about the NS EOS, and could be easier to detect with broadband interferometers than NS–NS merger signals (Vallisneri 2000).

A systematic study of BH–NS binary mergers will require exploration of a parameter space much larger than for NS–NS binaries. In particular, a wide range of mass ratios should be considered,  $q = M_h/M_{ns} \simeq 1 - 20$ , since BH masses are not expected to be concentrated in a narrow range (observations of BH X-ray binaries suggest  $M_h \simeq 5 - 15 M_\odot$ , but this may be biased by observational selection effects). Newtonian results suggest that for very low-mass BH ( $q \simeq 1$ ) the NS is quickly disrupted after the system reaches the ISCO, while for more massive BH ( $q \gtrsim 5$ ) the behavior is more erratic and complete tidal disruption of the NS may only occur after a large number of orbital periods and repeated brief episodes of mass transfer (Davies, Levan, & King 2005). In most cases, roughly one third of the NS mass is left in a thick torus around the BH while the rest is quickly accreted. While these results may be (at best) qualitatively correct, it is clear that relativistic effects must play an important role in the evolution. For a massive BH in particular, the tidal disruption of the NS takes place entirely in a strong field region (see Sec. 4).

Although this paper will focus on the GW aspects of the binary coalescence problem, the astrophysical motivation for the study of this problem is much broader. The ejection of nuclear matter during mergers has been discussed as a possibly major source of heavy “r-process” elements in galaxies (Lattimer & Schramm 1974; Rosswog, Freiburghaus, & Thielemann 2001). Many theoretical models of gamma-ray bursts (GRBs) have also relied on coalescing compact binaries to provide the energy of GRBs at cosmological distances (e.g., Eichler et al. 1989; Narayan, Paczyński, & Piran 1992; Mészáros & Rees 1992). Currently these models all assume that the coalescence leads to the formation of a rapidly rotating Kerr BH surrounded by a torus of debris (e.g., van Putten & Levinson 2002). Energy can then be extracted either from the rotation of the BH or from the material in the torus so that, with sufficient beaming, the gamma-ray fluxes observed from even the most distant GRBs could be explained. Here also, it is important to understand the hydrodynamic processes taking place during the final coalescence before making assumptions about its outcome. For example, contrary to widespread belief, it is not clear that the coalescence of two  $1.4 M_\odot$  NS will form an object that must collapse to a BH (Sec. 3).

## 2 Smoothed Particle Hydrodynamics

The hydrodynamic calculations of compact binary coalescence described below in Sec. 3 and 4 were done using two different relativistic smoothed particle hydrodynamics (SPH) codes, which we will refer to as the “Northwestern code” and the “Penn State code.” SPH is a Lagrangian, particle-based method ideally suited to calculations involving self-gravitating fluids moving freely in 3D.

Because of its Lagrangian nature, SPH presents some clear advantages over more traditional grid-based methods for calculations of stellar interactions. Most importantly, fluid advection, even for stars with a sharply defined surface such as NSs, is accomplished without difficulty in SPH, since the particles simply follow their trajectories in the flow. In contrast, to track accurately the orbital motion of two stars across a large 3-D grid can be very difficult, and sharp stellar surfaces often require a special treatment (to avoid “bleeding”). SPH is also very computationally efficient, since it concentrates the numerical elements (particles) where the fluid is at all times, not wasting any resources on empty regions of space. For this reason, with given computational resources, SPH can provide higher averaged spatial resolution than grid-based calculations, although Godunov-type schemes such as PPM typically provide better resolution of shock fronts. This is certainly not a decisive advantage for binary coalescence calculations, where no strong shocks ever develop. SPH also makes it easy to track the hydrodynamic ejection of matter to large distances from the central dense regions. Sophisticated nested-grid algorithms are necessary to accomplish the same with grid-based methods.

The first relativistic version of the Northwestern code (using PN gravity) was developed by Faber & Rasio (2000, 2002). For a detailed description of the purely hydrodynamic aspects of this code, including the results of many test calculations, see Lombardi et al. (1999). In addition to binary coalescence problems this code has also been used extensively in Newtonian gravity to study many problems related to stellar collisions in dense star clusters (e.g., Sills et al. 2001). Our current relativistic version of the code is based on the CF approximation to full GR (Faber et al. 2004). We solve the elliptic field equations using spectral methods. Specifically, our SPH code was coupled to the software developed by the Meudon group, which is publicly available as part of the C++ LORENE library ([www.lorene.obspm.fr](http://www.lorene.obspm.fr)). In contrast to finite-difference schemes, the fields are represented in terms of expansions over analytic basis functions. The effects of all operators, such as derivatives, are then represented by matrix multiplication on the coefficients of the expansion. In LORENE, the tensorial basis of decomposition is Cartesian, but each component is given in terms of spherical coordinates. In the current version, the usual basis of decomposition contains trigonometric polynomials or spherical harmonics for the dependence on the angles and Chebyshev polynomials for the dependence on the radial coordinate (Bonazzola et al. 1999).

The original version of the Penn State code is described by Laguna, Miller, & Zurek (1993). This code models relativistic fluid flow in a *fixed* curved spacetime geometry assuming that (a) the background spacetime is static (e.g., Schwarzschild or Kerr BH), and (b) the density of mass-energy of the fluid is sufficiently small that a Newtonian model of the fluid’s self-gravity is an adequate approximation. The code was calibrated with several 1-D benchmarks (Laguna et al. 1993) such as relativistic shock tubes, dust infall onto a BH, and Bondi collapse. It has been used recently to study the tidal disruption of main sequence stars by a supermassive BH (Laguna et al. 1993b; Kobayashi et al. 2004). For our BH–NS merger calculations we use the Kerr-Schild form of the Kerr (or Schwarzschild) metric to describe a fixed background. The coordinates smoothly penetrate the horizon of the holes, and they are suitable for studying the evolution of stars orbiting closely around the horizon or even falling into it. An absorbing boundary is set up well inside the horizon, and SPH particles crossing this boundary are removed from the calculation before they hit the BH singularity. This ensures a long-term, stable numerical evolution of the system. For obvious reasons this code should apply most accurately to BH–NS binaries in which the BH mass is much larger than the NS mass.

### 3 Neutron Star Binaries

A typical NS–NS binary merger, calculated with the Northwestern SPH code in CF gravity, is illustrated in Fig. 1 (from Faber et al. 2004). The initial phase of the evolution corresponds to the end of the binary inspiral, but with finite-size effects becoming important. In particular, a significant “tidal lag” (misalignment of the stellar long axes with respect to the binary axis) develops before contact. When physical merging begins, the two stars come together in an off-axis manner, with a very small amount of mass running along the surface interface before being spun off the newly forming remnant. This small amount of ejected matter, representing less than 1% of the total system mass in this particular calculation, remains gravitationally bound, forming a tenuous halo around the rapidly and differentially rotating remnant, which is stable to gravitational collapse.

We calculate the GW signal produced during the merger in the lowest-order quadrupole limit, finding

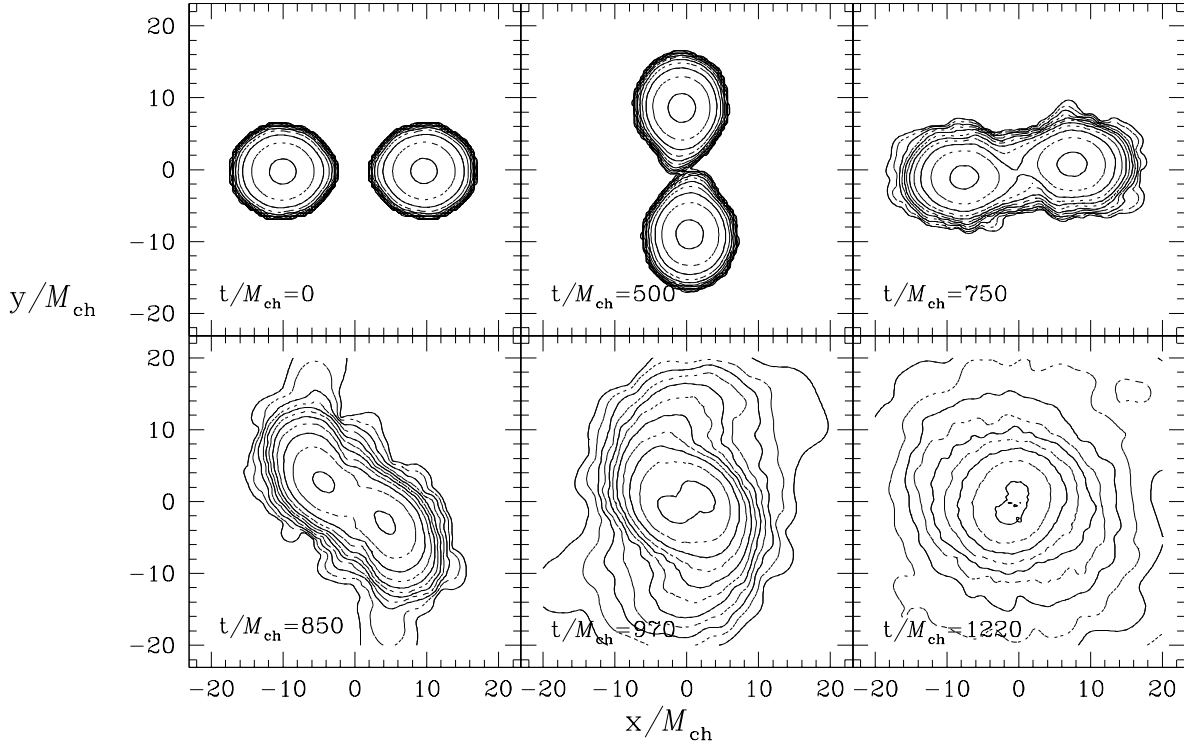


Figure 1: Final merger of a NS–NS binary. Units are defined such that  $G = c = 1$ , and  $M_{\text{ch}}$  is the chirp mass of the system. Density contours are shown in the equatorial ( $x - y$ ) plane of the system, logarithmically spaced with two contours per decade. We first see the development of significant tidal lag, followed by an “off-center collision” that leads to the formation of a vortex sheet at the interface between the two stars and a small amount of matter ejection. The final configuration is a very rapidly and differentially rotating, spheroidal NS, which is stable against gravitational collapse. This calculation was performed using  $10^5$  SPH particles in the CF approximation of GR. The initial condition consists of two identical, non-spinning (irrotational) NSs with a  $\Gamma = 2$  polytropic EOS, in a quasi-equilibrium circular orbit outside the ISCO. The orbital rotation is in the counter-clockwise direction.

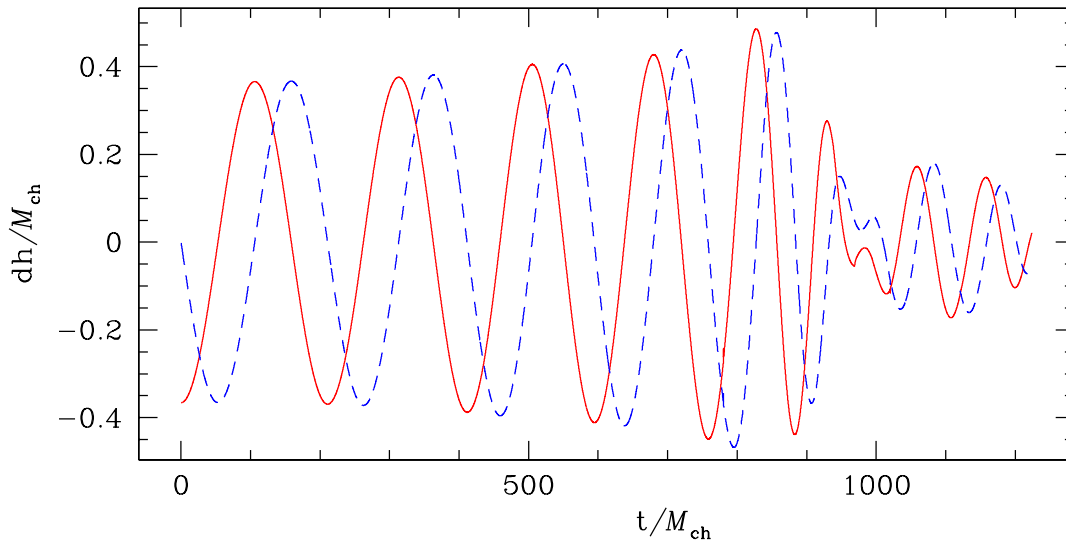


Figure 2: Gravitational wave signal in the  $h_+$  (solid line) and  $h_\times$  (dashed line) polarizations, for an observer located a distance  $d$  from the system along the rotation axis. Units are as in Fig. 1. We see the end of the inspiral chirp signal, followed by a lower-amplitude, modulated burst of high-frequency emission during the final merger.

good agreement with other recent relativistic calculations (Faber et al. 2004). Prior to final merger, we observe a “chirp” signal, as the frequency and amplitude both increase while the two NSs approach each other. After the merger, there is a period of strong, modulated high-frequency emission, which damps away as the remnant relaxes toward a spheroidal shape.

While the time-dependence of the GW signal is important, it is more useful in practice to look at the frequency dependence of the signal, and, in particular, the energy spectrum  $dE_{\text{GW}}/df$ . Indeed, one can show (Faber et al. 2002) that the changes in the total energy along quasi-equilibrium binary configurations for NS models with different compactness values  $M/R$  should leave an imprint in the energy spectrum in the form of a “break,” where the spectrum plunges rapidly below the power-law extrapolation of the low-frequency, slow inspiral spectrum ( $dE_{\text{GW}}/df \propto f^{-1/3}$ ). This corresponds to the sudden acceleration of the orbital decay as the NS binary approaches the point of onset of dynamical instability along a quasi-equilibrium sequence (Lai, Rasio, & Shapiro 1994; Lombardi et al. 1997). This is potentially detectable by narrow-band detectors in advanced interferometers. Using a parameterized model of these “break frequencies,” Hughes (2002) showed that the NS radius could be determined to within a few percent with at most  $\sim 50$  Advanced LIGO observations of NS mergers, and perhaps far fewer for optimal parameter values.

Since our calculation was started from a proper quasi-equilibrium initial condition, we can easily attach the inspiral waveform onto our calculated merger waveform at the point where the binary reaches the correct infall velocity. We note, however, that the exact point where the crossover is made has virtually no effect on the resulting spectrum. In Fig. 3, we show (as the solid line) a complete and *self-consistent* relativistic spectrum for a binary NS merger. At low frequencies, the primary contribution is from the inspiral signal, and at high frequencies, from the calculated merger waveform. The short-dashed line shows the Newtonian power-law result for two point masses, and the long-dashed curve shows the fit we find from our quasi-equilibrium sequence data (following Faber et al. 2002). We see excellent agreement up until the peak at frequencies around  $M_{\text{ch}}f_{\text{GW}} \simeq 0.007 - 0.009$ . This peak represents the “piling up” of energy corresponding to the moment when the stars make contact and the radial infall rate slows down in response to pressure building up. The second peak, at  $M_{\text{ch}}f_{\text{GW}} \simeq 0.010 - 0.011$ , represents emission from the ringdown of the merger remnant. It is likely that we underestimate the true height of this second peak somewhat, since we assume that the GW signal after our calculation ends continues to damp away exponentially, but the detection of this high-frequency peak will be quite challenging anyway.

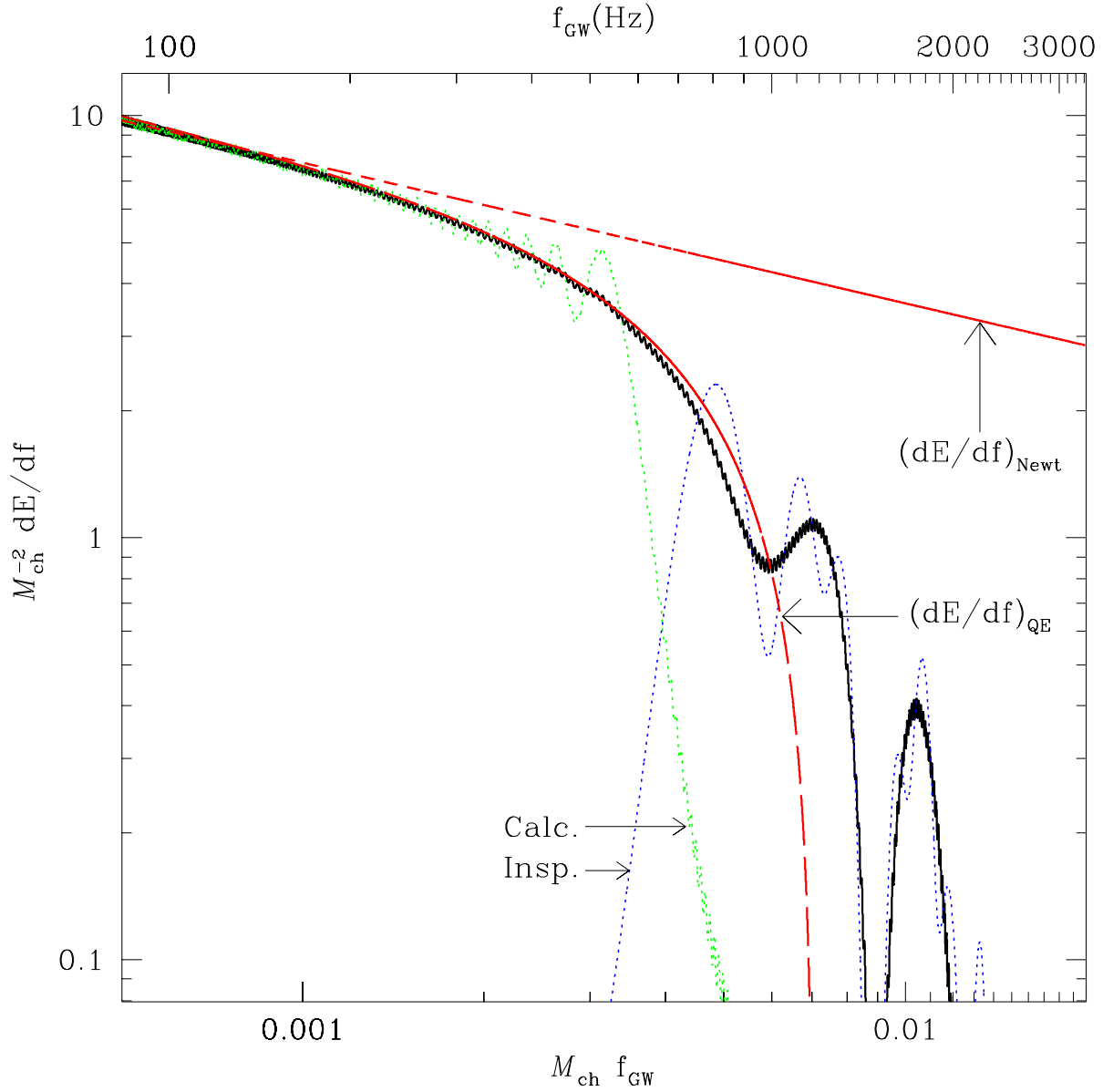


Figure 3: Gravitational wave energy spectrum,  $dE/df$ , as a function of GW frequency,  $f_{\text{GW}}$ . Units are defined such that  $G = c = 1$ , and  $M_{\text{ch}}$  is the chirp mass of the system. The dotted lines at high and low frequencies show the components contributed by our calculated signal and the quasi-equilibrium inspiral component, respectively. Also shown are the Newtonian point-mass energy spectrum (short-dashed line), and the semi-analytic result derived from a quasi-equilibrium binary NS sequence (long dashed line; Faber et al. 2002). On the upper horizontal axis, we also show the corresponding frequencies in Hz assuming that each NS has a mass of  $1.4 M_{\odot}$ . We see that the “break frequency” occurs well below  $\sim 1$  kHz, where ground-based interferometers retain good sensitivity (above  $\sim 1$  kHz laser shot noise leads to a rapid loss of sensitivity).

The final fate of a NS–NS merger depends crucially on the NS EOS, and on the extraction of angular momentum from the system during the final merger. For a stiff NS EOS, it is by no means certain that the core of the final merged configuration would collapse on a dynamical timescale to form a BH. One reason is that the Kerr parameter  $a/M$  of the core may exceed unity for an extremely stiff EOS (Baumgarte et al. 1998), although recent hydrodynamic calculations suggest that this is never the case (see, e.g., Faber & Rasio 2000). More importantly, the rapidly rotating core may in fact be dynamically stable. Take the obvious example of a system containing two identical  $1.4 M_{\odot}$  NSs. The total baryonic mass of the system for a stiff NS EOS is then about  $3 M_{\odot}$ . Most modern (stiff) nuclear EOS allow stable, maximally rotating NS with baryonic masses exceeding  $3 M_{\odot}$  (Cook, Shapiro, & Teukolsky 1994), i.e., above the mass of the final merger core, even if we entirely neglect fluid ejection. *Differential* rotation can further increase this maximum stable mass very significantly (Baumgarte, Shapiro, & Shibata 2000). Using realistic nuclear EOS, Morrison, Baumgarte, & Shapiro (2004) show that the merger remnants of all NS binaries observed in our Galaxy as binary pulsars could be supported stably against prompt collapse by rapid differential rotation. Recent full GR calculations of NS binary mergers in 3-D numerical relativity have also suggested that at least some merger remnants with stiff EOS are stable to collapse (Shibata, Taniguchi, & Uryu (2003).

However, for slowly rotating stars, the same EOS give maximum stable baryonic masses in the range  $2.5 - 3 M_{\odot}$ . Thus the final fate of the merger depends critically on its rotational profile and total angular momentum. Many processes such as electromagnetic radiation, neutrino emission, or the development of various secular instabilities (e.g., r-modes), which may also lead to angular momentum losses, take place on timescales much longer than the dynamical timescale (see, e.g., Baumgarte & Shapiro 1998, who show that neutrino emission is probably negligible). These processes are therefore decoupled from the hydrodynamics of the merger. Unfortunately their study is plagued by many fundamental uncertainties in the microphysics. Duez et al. (2004) have demonstrated for the first time in full GR how viscosity and magnetic fields can drive a differentially rotating, “hypermassive” NS merger remnant toward uniform rotation, possibly leading to delayed collapse to a BH. This delayed collapse would be accompanied by a secondary burst of GW.

The question of the final fate of the merger also depends crucially on the evolution of the fluid vorticity during the coalescence. Close NS binaries are likely to be *nonsynchronized*. Indeed, the tidal synchronization time is almost certainly much longer than the orbital decay time (Kochanek 1992; Bildsten & Cutler 1992). For NS binaries that are far from synchronized, the final coalescence involves complex hydrodynamic processes (Rasio & Shapiro 1999). In the simple case of an irrotational system (containing stars that are non-spinning at large separation), the two sides appear to be counter-spinning in the corotating frame of the binary. At the moment of first contact, a *vortex sheet* is formed. Such a vortex sheet is Kelvin-Helmholtz unstable on all wavelengths and the hydrodynamics is therefore very challenging to model accurately given the limited spatial resolution of 3-D calculations (see Faber & Rasio 2002 for a high-resolution SPH calculation using  $10^6$  particles and focusing on this aspect of the problem).

The final fate of the merger could depend crucially on the evolution of this shear flow inside the merging stars. In particular, if the shear persists and can support a highly triaxial shape for the remnant, a much larger fraction of the total angular momentum of the system could be radiated away through GW emission. In this case the final merged core may resemble a Dedekind ellipsoid, i.e., it will have a triaxial shape supported entirely by internal fluid motions, but with a stationary shape in the inertial frame (so that it no longer radiates GWs). The stability of such a configuration to gravitational collapse has never been studied. In contrast, in all 3-D numerical simulations performed to date, the shear is quickly dissipated, so that GW emission never gets a chance to extract more than a small fraction ( $\sim 10\%$ ) of the angular momentum, and the final core appears to be nearly axisymmetric. However, this behavior could be an artefact of the spurious shear viscosity present in all 3-D simulations.

## 4 Black Hole – Neutron Star Mergers

We now turn to BH–NS binaries, summarizing some recent (and rather preliminary) results we have obtained with the Penn State SPH code. Fig. 4 shows why the final merger of a BH–NS binary (for a typical stellar-mass BH) is particularly interesting but also particularly difficult to compute: the tidal (Roche) limit is typically right around the ISCO and the BH horizon. On the one hand, this implies

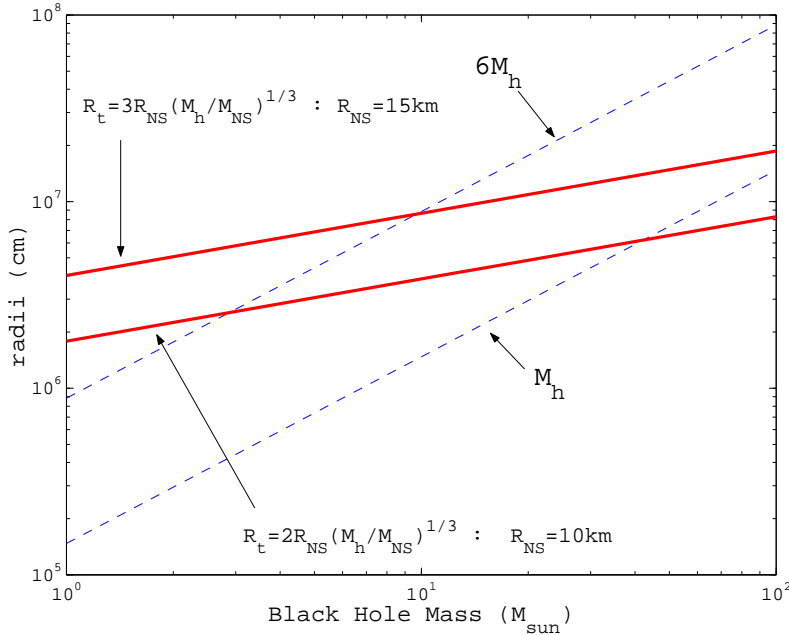


Figure 4: Tidal disruption limits for a  $1.4 M_{\odot}$  NS in circular orbit around a BH of mass  $M_h$ . The radius of the innermost stable circular orbit (ISCO) is also shown for the Schwarzschild and maximally corotating Kerr cases (dashed lines). The two solid lines bracket the Roche limit for NS with different spins and radii.

that careful, fully relativistic calculations are needed. On the other hand, it also means that the fluid behavior and the GW signals could depend sensitively (and carry rich information) on both the masses and spins of the stars, and on the NS EOS. How much information is carried about the fluid depends on where exactly the tidal disruption of the NS occurs: for a sufficiently massive BH, the horizon will always be encountered well outside the tidal limit, in which case the NS behavior remains point-like throughout the merger.

We set up initial conditions for BH–NS binaries near the Roche limit using the Penn State SPH code and a relaxation technique similar to those used for previous SPH studies of close binaries (e.g., Rasio & Shapiro 1995). First we construct hydrostatic equilibrium NS models for a simple gamma-law EOS by solving the Lane-Emden equation. When the NS with this hydrostatic profile is placed in orbit near a BH, spurious motions could result as the fluid responds dynamically to the sudden appearance of a strong tidal force. Instead, the initial conditions for our dynamical calculations are obtained by relaxing the NS in the presence of a BH in the corotating frame of the binary. For *synchronized* configurations (assumed here), the relaxation is done by adding an artificial friction term to the Euler equation of motion in the corotation frame. This forces the system to relax to a minimum-energy state. We numerically determine the angular velocity  $\Omega$  corresponding to a circular orbit at a given  $r$  as part of the relaxation process. The advantage of using SPH itself for setting up equilibrium solution is that the dynamical stability of these solutions can then be tested immediately by using them as initial conditions for dynamical calculations.

We illustrate our results from two simulations using  $10^4$  SPH particles to represent a NS with a  $\Gamma = 2$  polytropic EOS. The only difference between these two simulations is in the assumed spin of the BH: maximally corotating (Kerr parameter  $a/M_h = 1$  and corotating NS in the equatorial plane) in one case; non-rotating (Schwarzschild BH) for the other. Snapshots of the SPH particles near the end of these simulations are shown in Figs. 5 and 6. Around the maximally rotating BH, the fluid forms a stable ring just outside the BH horizon, while for the non-spinning BH the entire mass of the NS disappears into the horizon and is accreted by the BH on a dynamical timescale. There are many obvious implications of these results for models of gamma-ray bursts, which depend crucially on the presence of an accretion disk or torus around the BH. We note also that, so far, we have never observed the behavior seen in Newtonian simulations, where “stable mass transfer” from the NS onto the BH can persist for many

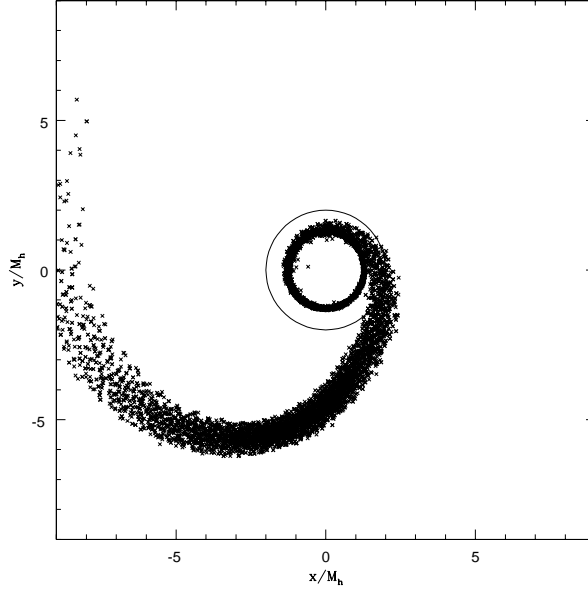


Figure 5: Tidal disruption of a  $1.4 M_{\odot}$  NS by a maximally corotating Kerr BH of mass  $M_h = 10 M_{\odot}$ . The NS was initially placed just outside the Roche limit ( $r \simeq 6.5 M_h$  for this NS of radius  $R \simeq 15$  km with a  $\Gamma = 2$  polytropic EOS). In this snapshot near the end of the simulation all SPH particles are shown projected onto the equatorial plane of the system. The NS has been completely disrupted, and a ring of material has formed just outside the BH horizon (at  $r = M_h$ ; the circle drawn for reference corresponds to  $r = 2 M_h$ ).

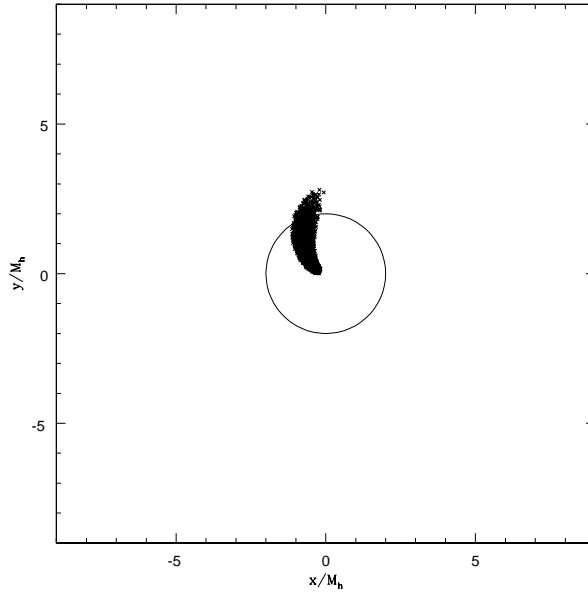


Figure 6: Same as in Fig. 5 but for a nonrotating (Schwarzschild) BH. Here again the NS has been completely disrupted, but the NS fluid is disappearing into the BH horizon (at  $r = 2 M_h$ , indicated by circle) and a stable ring of matter cannot form around the BH. Note that our inner absorbing boundary is located at  $r = 0.2 M_h$ , well inside the horizon.

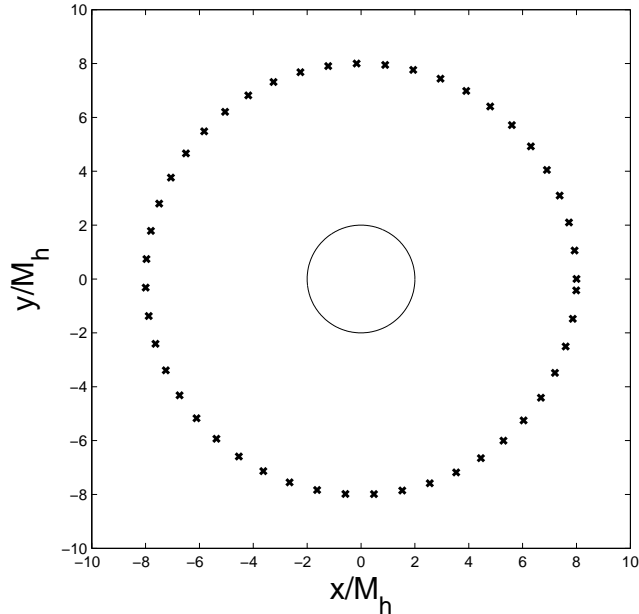


Figure 7: Test calculation for a WD orbiting a much more massive BH at  $r = 8 M_h$ . The mass ratio in this case is  $q \simeq 4 \times 10^5$ . The constant radius of this circular orbit is maintained by our code to within better than  $10^{-3}$  over one full period. Here each cross indicates the position of the WD (center of mass of all SPH particles) at a different time along the orbit (counter-clockwise).

orbits. Although our calculations so far have been for initial circular orbits in the equatorial plane of a Kerr BH, this is probably not realistic for most BH-NS binaries, where the NS is formed second, with a kick that would have likely tilted the plane of the orbit with respect to the BH spin (Kalogera 2000).

We have also performed several test calculations for white dwarfs (WDs) orbiting stably around a much more massive BH near their Roche limits. In this case the mass ratio is extreme, and our approximation (moving the fluid on a fixed background metric) should be nearly exact. For example, if we place a  $0.6 M_\odot$  WD in orbit around a Schwarzschild BH with  $M_h = 2 \times 10^5 M_\odot$ , we find that we can maintain a circular orbit at  $r = 8 M_h$  to within  $|\Delta r|/r < 10^{-3}$  over one full orbital period. This is illustrated in Fig. 7.

## Acknowledgements

This work was supported by NSF Grant PHY-0245028 at Northwestern University. SK and PL acknowledge support from the Eberly Research Funds of Pennsylvania State University, the Center for Gravitational Wave Physics, funded under NSF cooperative agreement PHY-0114375, and a NASA Swift Cycle 1 GI program. FR also thanks the Center for Gravitational Wave Physics for hospitality and support. JF is supported by an NSF Postdoctoral Fellowship in Astronomy and Astrophysics at UIUC.

## References

- [1] Ayal, S., Piran, T., Oechslin, R., Davies, M.B., Rosswog, S. 2001, ApJ, 550, 846
- [2] Baumgarte, T.W., & Shapiro, S.L. 1998, ApJ, 504, 431
- [3] Baumgarte, T.W., Cook, G.B., Scheel, M.A., Shapiro, S.L., & Teukolsky, S.A. 1998, PRD 57, 7299
- [4] Baumgarte, T.W., Shapiro, S.L., & Shibata, M. 2000, ApJ, 528, L29

- [5] Baumgarte, T.W., Skoge, M.L., & Shapiro, S.L. 2004, PRD, 70, 064040
- [6] Bildsten, L., & Cutler, C. 1992, ApJ, 400, 175
- [7] Blanchet, L., Damour, & Schäfer, G. 1990, MNRAS, 242, 289
- [8] Bonazzola, S., Gourgoulhon, E., & Marck, J.-A. 1999, J. Comp. Appl. Math., 109, 433
- [9] Cook, G.B., Shapiro, S.L., & Teukolsky, S.A. 1994, ApJ, 424, 823
- [10] Damour, T., Gourgoulhon, E., & Grandclément, P. 2002, PRD, 66, 024007
- [11] Davies, M.B., Levan, A.J., & King, A.R. 2005, MNRAS, 356, 54
- [12] Duez, M.D., Liu, Y.T., Shapiro, S.L., Stephens, B.C. 2004, PRD, 69, 104030
- [13] Eichler, D., Livio, M., Piran, T., & Schramm, D.N. 1989, Nature, 340, 126
- [14] Faber, J.A., & Rasio, F.A. 2000, PRD, 62, 064012
- [15] Faber, J.A., & Rasio, F.A. 2002, PRD, 65, 084042
- [16] Faber, J.A., Grandclément, P., Rasio, F.A., & Taniguchi, K. 2002, PRL, 89, 231102
- [17] Faber, J.A., Grandclément, P., & Rasio, F.A. 2004, PRD, 69, 124036
- [18] Grandclément, P., Gourgoulhon, E., & Bonazzola, S. 2002, PRD, 65, 044021
- [19] Hughes, S.A. 2002, PRD, 66, 102001
- [20] Ishii, M., Shibata, M., & Mino, Y. 2005, PRD, 71, 044017
- [21] Kalogera, V. 2000, ApJ, 541, 319
- [22] Kobayashi, S., Laguna, P., Phinney, E.S., & Meszaros, P. 2004, ApJ, 615, 855
- [23] Kochanek, C.S. 1992, ApJ, 398, 234
- [24] Laguna, P., Miller, W.A. & Zurek, W.H. 1993a, ApJ, 404, 678
- [25] Laguna, P., Miller, W.A., Zurek, W.H. & Davies, M.B. 1993b, ApJ, 410, L83
- [26] Lai, D., Rasio, F.A., & Shapiro, S.L. 1994, ApJ, 420, 811
- [27] Lattimer, J.M., & Schramm, D.N. 1974, ApJ, 192, L145
- [28] Lee, W.H. 2001, MNRAS, 328, 583
- [29] Lombardi, J.C., Rasio, F.A., & Shapiro, S.L. 1997, PRD, 56, 3416
- [30] Lombardi, J.C., Sills, A., Rasio, F.A., & Shapiro, S.L. 1999, J. Comp. Phys., 152, 687
- [31] Mathews, G.J., Marronetti, P., & Wilson, J.R. 1998, PRD, 58, 043003
- [32] Mészáros, P., & Rees, M.J. 1992, ApJ, 397, 570
- [33] Miller, M., Gressman, P., & Suen, W. 2004, PRD, 69, 064026
- [34] Morrison, I.A., Baumgarte, T.W., & Shapiro, S.L. 2004, ApJ, 610, 941
- [35] Nakamura, T. 1994, in Relativistic Cosmology, ed. M. Sasaki (Universal Academy Press), 155
- [36] Narayan, R., Paczyński, B., & Piran, T. 1992, ApJ, 395, L83
- [37] Oechslin, R., Rosswog, S., Thielemann, F. 2002, PRD 65, 103005

- [38] Oohara, K., & Nakamura, T. 1992, Prog. Th. Phys., 88, 307
- [39] Rasio, F.A., & Shapiro, S.L. 1995, ApJ, 438, 887
- [40] Rasio, F.A., & Shapiro, S.L. 1999, CQG, 16, 1
- [41] Rosswog, S., Freiburghaus, C., & Thielemann, F.-K. 2001, Nucl. Phys. A, 688, 344
- [42] Shibata, M. 1997, PRD, 55, 6019
- [43] Shibata, M., & Uryu, K. 2000, PRD, 61, 064001
- [44] Shibata, M., & Uryu, K. 2001, PRD, 64, 104017
- [45] Shibata, M., & Sekiguchi, Y. 2004, 69, 084024
- [46] Shibata, M., Taniguchi, K., & Uryu, K. 2003, PRD, 68, 084020
- [47] Sills, A., Faber, J.A., Lombardi, J.C., Rasio, F.A., & Warren, A. 2001, ApJ, 548, 323
- [48] Vallisneri, M. 2000, PRL, 84, 3519
- [49] van Putten, M.H.P.M., & Levinson, A. 2002, Science, 295, 1874
- [50] Wilson, J.R., Mathews, G.J., & Marronetti, P. 1996, PRD, 54, 1317